A Journal of the Gesellschaft Deutscher Chemiker

Angewandte International Edition GDCh Chemie

www.angewandte.org

## Accepted Article

**Title:** A Multifluorination Strategy Toward Wide Bandgap Polymers for Highly Efficient Organic Solar Cells

**Authors:** Jinming Chen, Dongyan Li, Mingbin Su, Yonghong Xiao, Hui Chen, Man Lin, Xiaolan Qiao, Li Dang, Xiao-Chun Huang, Feng He, and Qinghe Wu



**To be cited as:** *Angew. Chem. Int. Ed.* **2023**, e202215930

**Link to VoR:** https://doi.org/10.1002/anie.202215930

WILEY-VCH

10.1002/anie.202215930

WILEY-VCH

RESEARCH ARTICLE

# A Multifluorination Strategy Toward Wide Bandgap Polymers for Highly Efficient Organic Solar Cells

Jinming Chen,[a,#] Dongyan Li,[a,#] Mingbin Su,[a] Yonghong Xiao,[a] Hui Chen,[b] Man Lin,[a] Xiaolan Qiao,[d] Li Dang, [a] Xiao-Chun Huang,[a,c] Feng He,[b,e] Qinghe Wu*[a,c]

[a] Prof. Q. Wu, Prof. X. Huang, Prof. L. Dang, J. Chen, D. Li, M. Su, Y. Xiao
Department of Chemistry and Key Laboratory for Preparation and Application of Ordered Structural Materials of Guangdong
Shantou University
Shantou, Guangdong 515063, China
E-mail: wuqh@stu.edu.cn
[b] Prof. F. He, H. Chen
Shenzhen Grubbs Institute and Department of Chemistry Southern University of Science and Technology
Shenzhen, 518055, China
[c] Prof. Q. Wu, Prof. X. Huang
Chemistry and Chemical Engineering Guangdong Laboratory
Shantou, 515063, China
[d] Prof. X. Qiao
State Key Laboratory for Modification of Chemical Fibers and Polymer Materials, College of Materials Science and Engineering
Donghua University
Shanghai 201620, China
[e] Prof. F. He
Guangdong Provincial Key Laboratory of Catalysis
Southern University of Science and Technology
Shenzhen, 518055, China
# These authors made equal contribution.

Supporting information for this article is given via a link at the end of the document.

**Abstract:** Creating new electron-deficient unit is highly demanded to develop high-performance polymer donors for non-fullerene organic solar cells (OSCs). Herein, we reported a multifluorinated unit 4,5,6,7-tetrafluoronaphtho[2,1-b:3,4-b']dithiophene (FNT) and its polymers PFNT-F and PFNT-Cl. The advantages of multifluorination: (1) it enables the polymers to exhibit low-lying HOMO (~ -5.5 eV) and wide bandgap (~ 2.0 eV); (2) the short interactions (F···H, F···F) endow the polymers with properties of high film crystallinity and efficient hole transport; (3) well miscibility with NFAs that leads to a more well-defined nanofibrous morphology and face-on orientation in the blend films. Therefore, the PFNT-F/Cl:N3 based OSCs exhibit impressive FF values of 0.80, and remarkable PCEs of 17.53 % and 18.10 %, which make them ranked the best donor materials in OSCs. This work offers new insights into the rational design of high-performance polymers by multifluorination strategy.

## Introduction

Currently, the dominating non-fullerene acceptors (NFAs) in organic solar cells (OSCs) are Y6 and its derivatives which have physical properties of 600 - 900 nm light absorption coverage, moderate HOMO energy level, and high crystallinity.[1] These new features demand polymer donors with matched physical properties, such as complementary light absorption, suitable HOMO energy level and excellent morphological compatibility.[2] However, very limited polymers could perfectly meet these requirements and how to design new polymers with desired properties remains challenging.[3] In D-A co-polymers, the electron-deficient unit significantly affects the photophysical and film-forming properties of the polymer,[4] For example, 3-fluorothieno[3,4-b]thiophene-2-carboxylate based PTB7-Th bears narrow bandgap,[5] benzo[1,2-c:4,5-c']dithiophene-4,8-dione based PM6 exhibits medium bandgap and high crystallinity.[6] Historically speaking, the electron-deficient unit played a crucial role in the evolution of state-of-the-art polymers.[4d, 7] Therefore, creating new electron-deficient unit is highly demanded to develop high-performance polymer donors for non-fullerene OSCs.

Owing to the strong electronegativity and small size, fluorine is very useful to tune polymers' frontier energy levels, film crystallinity and charge carrier mobility.[7-8] Previously, introducing one or two fluorine atoms in electron-deficient units has created many well-known monomers for polymer donors as shown in Figure 1a.[5a, 8g-i] Compared with these monomers with fluorine and other conjugated electron-withdrawing groups, solely multifluorine substituted unit has its own advantages to construct polymers by matching with the broadly used NFAs because of the following reasons: (1) withdrawing electron by induction endow the polymer with wide bandgap which match well with visible-NIR NFAs;[7, 9] (2) the strong electron-withdrawing ability and short interactions of fluorine atom with other atoms enable the polymer exhibiting low-lying HOMO and high hole mobility, which would result in high $V_{oc}$ and FF values;[10] (3) multifluorinated polymers potentially benefit the miscibility with multifluorinated NFAs because the fluorine could drive intermolecular interactions,[10a, 10c, 11] which probably leads to favorable blend film morphology. Therefore, multifluorine substitution should be an effective way to create ideal electron-deficient monomers. However, the solely multifluorinated unit has not been developed for polymer donors to match with Y6 and its derivatives.

Based on the above consideration, we synthesized a novel multifluorinated unit 4,5,6,7-tetrafluoronaphtho[2,1-b:3,4-b']dithiophene (FNT) and developed the polymers PFNT-F and PFNT-Cl by copolymerizing with (4,8-bis(4-fluoro-5-(2-hexyldecyl)thiophen-2-yl)benzo[1,2-b:4,5-b']dithiophene-2,6-diyl)bis(trimethylstannane) and (4,8-bis(4-chloro-5-(2-hexylde-cyl)thiophen-2-

10.1002/anie.202215930




yl)benzo[1,2-b:4,5-b']dithiophene-2,6-diyl)bis(tri-methylstannane). The short π-π stacking distance of 3.38 Å and abundant short interactions (F···H, F···F) of FNT could favor the hole transport. The solely multifluorine substitutions enable both polymers to exhibit low-lying HOMO (~ -5.5 eV) and wide band gap (~ 2.0 eV) which perfectly match with photophysical properties of visible-NIR NFAs. Moreover, excellent morphological compatibility between PFNT-F/Cl and N3 (chemical structure in Scheme S3) leads to more well-defined nanofibrous structure and face-on orientation of both polymers in the blend films while mainly edge-on in the neat films. Finally, PFNT-F/Cl:N3 based OSCs exhibit impressively high FF values of 0.80, as well as remarkable PCEs of 17.53 % and 18.10 %, which make PFNT-F/Cl ranked the best polymer donors in non-fullerene OSCs. The slightly higher PCEs of PFNT-Cl could be attributed to its smaller radiative and non-radiative recombination energy losses. This study not only provides a promising electron-deficient unit FNT, but also suggests an efficient multifluorination strategy to rationally design high-performance polymers for OSCs.

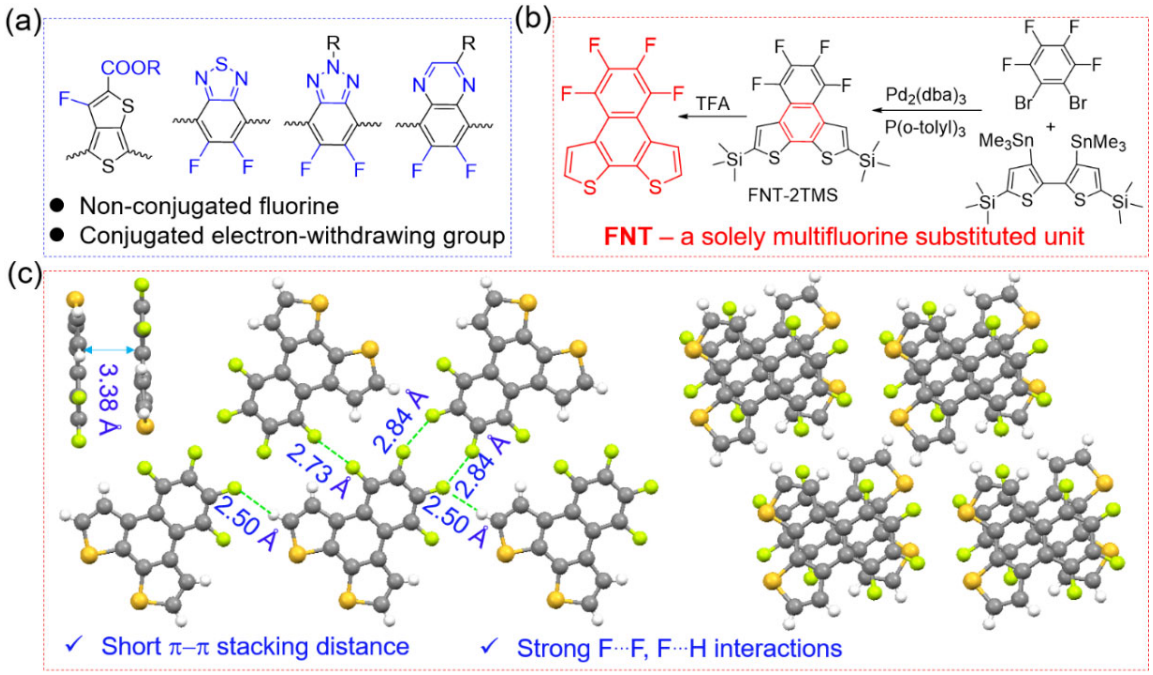


**Figure 1.** (a) The electron-deficient units with fluorine and other conjugated electron-withdrawing groups; (b) The chemical structure and synthesis of FNT; (c) The single crystal data of FNT, including π-π stacking, short interactions and molecular packing information.

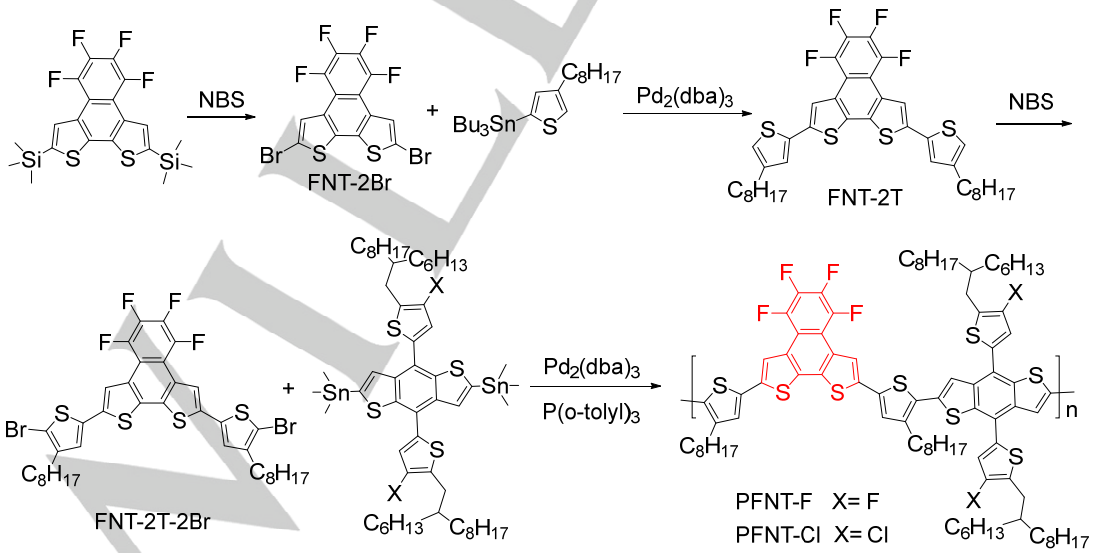


**Scheme 1.** Synthetic route of FNT-based polymer donors PFNT-F and PFNT-Cl.

## Results and Discussion

**Synthesis of monomers and polymers.** Introducing fluorine into a conjugated backbone usually requires tedious multi-step reactions.[5a, 6a] Taking the advantage of easily accessible tetrafluorinated compounds, it is a good choice to easily synthesize multifluorine substituted building units. From 1,2-dibromo-3,4,5,6-tetrafluorobenzene, we successfully synthesized

10.1002/anie.202215930

WILEY-VCH

RESEARCH ARTICLE

a multifluorine substituted compound 2,9-bis(tri-methylsilane)-4,5,6,7-tetrafluoronaphtho[2,1-b:3,4-b']dithiophene (FNT-2TMS) by Stille coupling with (3,3'-bis(tri-methylstannyl)-[2,2'-bithiophene]-5,5'-diyl)bis(trimethylsilane), which is a new and efficient method to construct six-membered aromatic ring by simple one-step reaction (Figure 1b). Further treating FNT-2TMS with trifluoroacetic acid, the 4,5,6,7-tetrafluoronaphtho[2,1-b:3,4-b']dithiophene (FNT) was obtained in high yield for single crystal analysis (Scheme S2).

The single crystal of FNT was cultivated by slow diffusion of ethanol into its chloroform solution. The short interactions and packing information are presented in Figure 1c, and crystal data information is summarized in Table S1. The molecule FNT shows good planarity with all atoms in the same plane. In the solid crystal, the FNT takes a slip-stacked head-to-tail packing with a π-π stacking distance of 3.38 Å. The very short π-π stacking distance implies the most electronegative atom fluorine could significantly reduce electron density on the surface of FNT. Two F···H interactions with the distances of 2.50 Å and 2.50 Å are observed in adjacent molecules. Importantly, more F···F interactions with short distances of 2.84 Å, 2.84 Å and 2.73 Å also exist. The F···F interactions could increase the miscibility of FNT-based polymers with multifluorine substituted NFAs (N3) because the fluorine drives intermolecular interactions, resulting in favorable morphology. The strong π-π stacking and abundant short interactions also favor the hole transport which makes FNT a very promising candidate for polymer donors.

After the bromination of FNT-2TMS, further Stille reaction and bromination generated monomer FNT-2T-2Br (Scheme 1). The polymers PFNT-F and PFNT-Cl were synthesized by Stille coupling of FNT-2T-2Br with (4,8-bis(4-fluoro-5-(2-hexyldecyl)thiophen-2-yl)benzo[1,2-b:4,5-b']dithioph-ene-2,6-diyl)bis(trimethyllstannane) and (4,8-bis(4-chloro-5-(2-hexyldecyl)thiophen-2-yl)benzo[1,2-b:4,5-b']dithiophene-2,6-diyl)bis(trimethylstannane), respectively. Both polymers have good solubility in hot solvents of chloroform and chlorobenzene. The gel permeation chromatography (GPC) measurement with trichlorobenzene as eluent at 150 °C yielded the molecular weight and dispersity of 29.9 kg/mol and 1.87 for PFNT-F, and 42.6 kg/mol and 1.97 and PFNT-Cl, respectively (Figure S1, 2). The thermogravimetric analysis (TGA) indicates both polymers demonstrate excellent thermal stability with decomposition temperature (5% weight loss) all over 400 °C (Figure S3). The differential scanning calorimetry (DSC) measurement shows no glass transition and melting peaks of PFNT-Cl and PFNT-F (Figure S4) at a scan range of 40 – 300 °C.

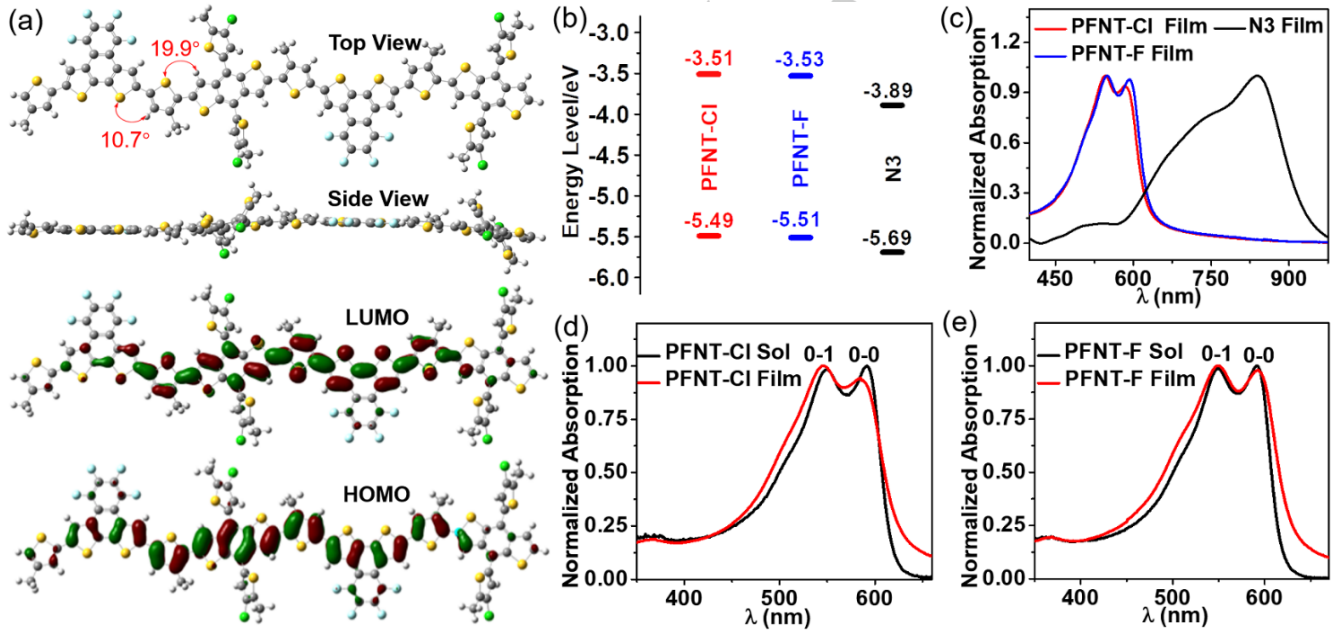


**Figure 2.** (a) The top/side view of calculated molecular geometries and LUMO/HOMO orbitals of two repeating units of PFNT; (b) Schematic frontier energy levels of PFNT-Cl, PFNT-F and N3; (c) The film absorption spectra of PFNT-Cl, PFNT-F and N3; (d) The absorption spectra of PFNT-Cl in solution and film; (e) The absorption spectra of PFNT-F in solution and film.

**Polymer Geometry Calculation.** The density functional theory using Gaussian package B3LYP/6-31G* was employed to investigate the polymer conjugated backbone planarity and frontier orbital distribution in two polymers. Because they have the same conjugated backbone except for Cl or F substitution in BDT, two repeating units of PFNT-Cl were used for calculation. To facilitate calculation, the long alkyl chains were replaced by methyl groups. The calculated molecular geometries and frontier orbital distributions are presented in Figure 2a. The LUMO and HOMO orbitals are all delocalized over the main conjugated chain of the polymer. The dihedral angles between FNT and thiophene, thiophene and BDT are 10.7° and 19.9°, respectively. Because of the good planarity of FNT and small dihedral angles, the polymer conjugated chain exhibits good long-range planarity (side view of calculated geometry), which benefits close π-π stacking (Figure 5) and efficient charge transport.

**Photophysical properties.** Cyclic voltammetry measurement was conducted to determine the frontier orbital energy level of PFNT-Cl and PFNT-F by using ferrocene (-4.80 eV) as standard reference (Figure S5). The $E_{LUMO}$ calculated from onset reduction potentials are -3.51 and -3.53 eV, while the $E_{HOMO}$ from onset oxidation are -5.49 and -5.51 eV for PFNT-Cl and PFNT-F, respectively. The low-lying HOMO energy levels of both polymers

10.1002/anie.202215930

WILEY-VCH

RESEARCH ARTICLE

indicate the strong electron-withdrawing ability of multifluorine substituted FNT. Additionally, the $\Delta E_{HOMO}$ offsets between two polymers and N3 are 0.20 and 0.18 eV which are enough to drive exciton dissociation in blend films. Both polymers have low-lying HOMO energy levels (~ -5.5 eV) and wide band gap (~ 2.0 eV) which match well with N3.

The UV-vis absorption of both polymers in film and solution was measured and presented in Figure 2c-e and Figure S6. Because both polymers have the same conjugated backbone except for the fluorine or chlorine substitution in BDT, nearly identical absorption spectra with two absorption peaks were observed in chloroform solution at a concentration of $5\times10^{-6}$ g/ml. The film of PFNT-F cast from the chloroform solution shows a 0-1 absorption peak at 550 nm that is nearly identical to that of the solution, and a slightly diminished 0-0 absorption peak at 592 nm. On the contrary, the 0-1 absorption peak of PFNT-Cl film is blue-shifted from 550 nm to 545 nm and more obviously weakened 0-0 absorption peak is blue-shifted from 592 nm to 585 nm. Because the molecular packing significantly affects the solid-state optical properties of π-conjugated materials,[12] the identical absorption spectra in solution and different absorption spectra in the film suggest PFNT-F and PFNT-Cl have different conjugated chains packing in the solid film. The temperature-dependent UV-vis spectra of PFNT-Cl and PFNT-F in chlorobenzene solution were measured and the data was summarized in Figure S7. The significant enhancement of 0-0 transition (that reflects π–π stacking of polymer chains) when lowering the temperature indicates strong polymer chains aggregation of both polymers in the solution.

We made the comparison of photophysical properties with the benchmark polymers PM6 and D18 (Figure S5, S8, the chemical structure in Scheme S2). The HOMO/LUMO, bandgap, maximum/onset absorption, and film absorption coefficient of four polymers were summarized in Table S2. The PFNT-F/Cl polymers exhibit slightly lower HOMO energy levels than D18 and PM6. The bandgaps and absorption end of PFNT-F/Cl are similar to D18, however, the 0-0 absorption peak lower than 0-1 in the film absorption spectra of both polymers is different from that for D18, which is probably caused by the molecular packing difference of the polymers.[13] The calculated film absorption coefficients (Figure S9) at absorption maximum are $5.24 \times 10^4$ $cm^{-1}$ for PFNT-F and $6.29 \times 10^4$ $cm^{-1}$ for PFNT-Cl, which are similar to $5.61\times10^4$ $cm^{-1}$ for PM6 and $5.64\times10^4$ $cm^{-1}$ for D18. Additionally, the film absorption range of both polymers (450 - 620 nm) complements 600 - 900 nm for N3 which benefits solar energy harvesting.

**Table 1.** *J-V* characteristics of PFNT-Cl and PFNT-F based solar cell devices and charge carrier mobility of blend films.

| Active layer | $V_{oc}$ [V] | $J_{sc}$ [mA $cm^{-2}$] | FF | PCE [%] (Aver.) [a] | $\mu_e$ ($cm^2V^{-1}S^{-1}$) | $\mu_h$ ($cm^2V^{-1}S^{-1}$) |
|---|---|---|---|---|---|---|
| PFNT-Cl:N3 | 0.853 | 26.56 | 0.799 | 18.10 (17.63±0.24) | $3.95\times10^{-4}$ | $4.37\times10^{-4}$ |
| PFNT-F:N3 | 0.842 | 26.03 | 0.800 | 17.53 (17.10±0.25) | $5.70\times10^{-4}$ | $4.07\times10^{-4}$ |

[a] The PCEs were obtained from over 30 devices.

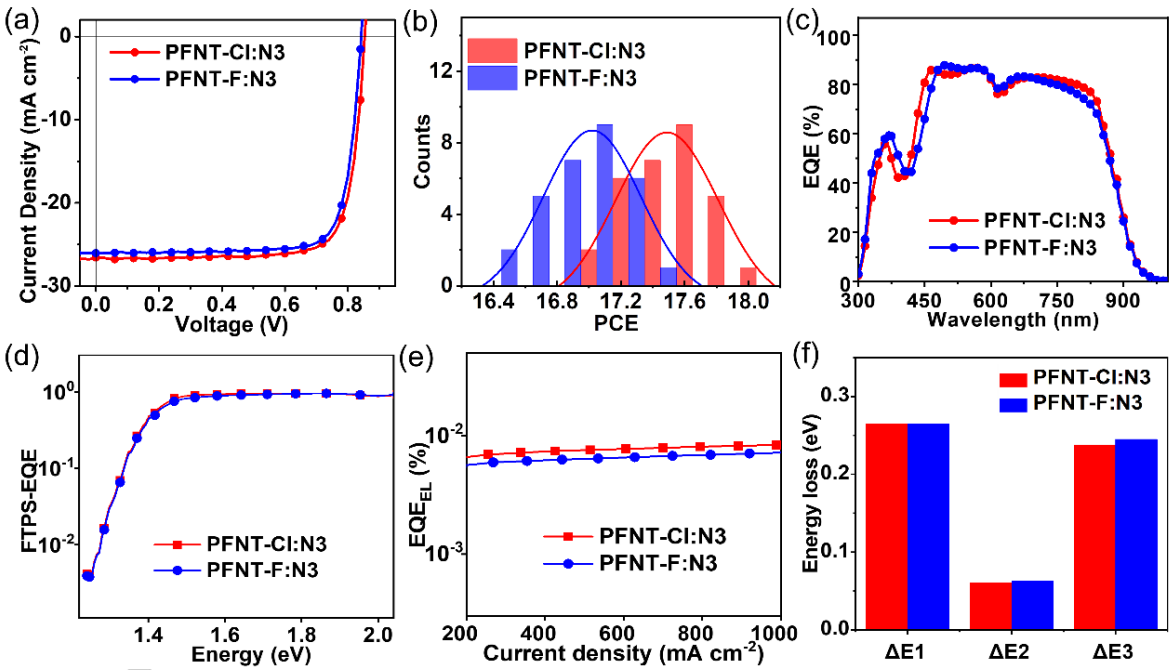


**Figure 3.** (a) The *J-V* curves, (b) Histogram of PCEs over 30 independent devices, (c) EQE spectra, (d) FTPS-EQE spectra, (e) $EQE_{EL}$ at different injection current density, (f) the schematic radiative and non-radiative recombination energy losses for PFNT-Cl:N3 and PFNT-F:N3 based OSCs.

**Photovoltaic properties.** The conventional devices with the configuration of ITO/PEDOT:PSS/PFNT-Cl or PFNT-F:N3/PNDIT-F3N/Ag were fabricated to investigate the photovoltaic properties of both polymers by using a narrow

10.1002/anie.202215930




bandgap N3 as electron acceptor[1c]. The OSC performance was measured under a simulated solar illumination of 100 mW $cm^{-2}$ AM 1.5G in a nitrogen-filled glovebox. By spin-coating their chloroform solution with a total concentration of 9.24 mg/ml and polymer/acceptor mass ratio of 1:1.2, the optimized blend films of two devices with thicknesses around 110 nm were obtained. The OPV parameters for PFNT-Cl/F:N3 based as-cast devices were summarized in Table S3. The best efficiency for PFNT-Cl:N3 and PFNT-F:N3 as-cast devices are 17.59 % and 16.69%, respectively. It was found that thermal annealing at 110 °C could effectively enhance the photovoltaic performance of devices. We presented the optimized photovoltaic parameters and *J-V* curves in Table 1 and Figure 3a. The highest efficiency of 18.10 % with $V_{OC}$ of 0.853 V, $J_{SC}$ of 26.56 mA $cm^{-2}$, and FF of 0.799 was obtained for PFNT-Cl:N3 based OSCs. The PFNT-F:N3 based device exhibits a slightly lower efficiency of 17.53 % with $V_{OC}$ of 0.842 V, a $J_{SC}$ of 26. 03 mA $cm^{-2}$, and FF of 0.800. A histogram of PCEs for over 30 independent devices was presented in Figure 3b. The efficiency is in a range between 16.5 % and 17.6 % for PFNT-F, and between 17.0 % and 18.1 % for PFNT-Cl. The decent photovoltaic performance of the two polymers indicates that multifluorinated FNT is a promising building unit for polymer donors. It should be noted that both polymers exhibit an impressive high FF value of 0.80. Currently, only polymers PM6 and PTQ10 exhibit the FF values over 0.80 and efficiencies higher than 18 % in binary OSCs.[1a, 14] The remarkable photovoltaic performances suggest that those new family of polymers are ranked the best donor materials in non-fullerene OSCs.

We measured the external quantum efficiency (EQE) of two devices and the spectra were demonstrated in Figure 3c. The calculated $J_{SC}$ from EQE is 25.82 mA $cm^{-2}$ for PFNT-Cl:N3 and 25.39 mA $cm^{-2}$ for PFNT-F:N3, which agree well with the $J_{SC}$ from *J-V* curves. The hole and electron mobility (Figure S10,11 and Table 1, Table S4) were measured by using the space-charge-limited-current (SCLC) method with a device structure of ITO/PEDOT:PSS/PFNT-Cl or PFNT-F:N3/$MoO_3$/Ag for hole mobility and ITO/ZnO/PFNT-Cl or PFNT-F:N3/PNDIT-F3N/Ag for electron mobility. The PFNT-Cl:N3 and PFNT-F:N3 exhibit similar hole mobility with values of 4.37 × $10^{-4}$ $cm^2V^{-1}s^{-1}$ and 4.07 × $10^{-4}$ $cm^2V^{-1}s^{-1}$, respectively. The electron mobility for PFNT-Cl:N3 and PFNT-F:N3 are 3.95 × $10^{-4}$ $cm^2V^{-1}s^{-1}$ and 5.70 × $10^{-4}$ $cm^2V^{-1}s^{-1}$, respectively. The balanced hole and electron mobility account for their high FF values. The hole mobility for neat PFNT-Cl and PFNT-F films are 3.74 × $10^{-4}$ $cm^2V^{-1}s^{-1}$ and 1.88× $10^{-4}$ $cm^2V^{-1}s^{-1}$, respectively. The lower hole mobility of PFNT-F could be explained by its edge-on orientation on the substrate (Figure 5). The higher hole mobility in blend film than in neat film is consistent with the molecular orientation changes from edge-on in neat film to face-on in blend film.

The exciton dissociation and charge separation properties of the two devices were investigated by measuring the photocurrent density ($J_{ph}$) as a function of effective voltage ($V_{eff}$) (Figure S12a).[15] The definition of charge dissociation probability *P(E, T)* is $J_{ph}/J_{sat}$; $J_{ph} = J_L - J_D$ ($J_L$ is light current density; $J_D$ is dark current density); $J_{sat}$ is defined as $J_{ph}$ reaches its saturation at high reverse voltage, where all the photogenerated excitons could be separated to free charges and collected by the electrodes. $V_{eff} = V_0 - V$ ($V_0$ is voltage where $J_{ph} = 0$). The calculated *P(E, T)* under $J_{SC}$ condition are 99 % and 98 % for PFNT-Cl:N3 and PFNT-F:N3 based devices, respectively, indicating the efficient exciton dissociation and charge separation at interfaces between polymers and acceptor. We evaluated the bimolecular recombination in the two devices by measuring the curve slope of $J_{SC}$ as a function of light intensity on a logarithmic scale (Figure S12b).[16] The calculated slope of the two devices are 0.99 and 0.98 for PFNT-Cl:N3 and PFNT-F:N3 which are close to 1, indicating the very weak bimolecular recombination in both devices.

**Energy loss study.** The polymer PFNT-Cl based device has a higher $V_{OC}$ value than that of PFNT-F. To understand the reason for their $V_{OC}$ difference, we studied the energy loss of the two devices by measuring the Fourier-transform photocurrent spectroscopy external quantum efficiency (FTPS-EQE) and $EQE_{EL}$ (Figure 3d, e, Figure S13). The optical bandgaps ($E_g$) for PFNT-Cl:N3 and PFNT-F:N3 are both 1.42 eV and calculated energy loss ($E_{loss}$) are 0.567 and 0.576 eV, respectively. The energy loss study regarding $E_g$, $\Delta E_1$, $\Delta E_2$ and $\Delta E_3$ was calculated from the following equation according to the reported work. [17]

$$E_{loss} = (E_g - qV_{oc}^{SQ}) + q\Delta V_{oc}^{rad} + q\Delta V_{oc}^{non-rad} = \Delta E_1 + \Delta E_2 + \Delta E_3$$

The $\Delta E_1$ that originates from radiative recombination loss above the band gap was calculated to be 0.265 eV for both devices. $\Delta E_2$ originates from radiative recombination loss below the gap, and PFNT-Cl based device shows a smaller $\Delta E_2$ value of 0.061eV while that for PFNT-F is 0.063 eV. The nonradiative recombination loss $\Delta E_3$ was calculated according to the equation: $\Delta E_3 = -k_BTln(EQE_{EL})$, and the values are 0.238 eV and 0.245 eV for PFNT-Cl:N3 and PFNT-F:N3 (Table S5). The smaller nonradiative recombination loss and radiative recombination loss below the gap account for the smaller energy loss of the PFNT-Cl:N3 based device, which explains their variation of $V_{OC}$.

**Morphological compatibility and molecular packing information.** The morphologies of neat polymer and blend films were studied by using the measurement of atomic force microscopy (AFM) and transmission electron microscopy (TEM). The phase images and TEM images were shown in Figure 4a-f and height images were presented in Figure S14, 15. The neat PFNT-F film has higher surface roughness with root-mean-square surface roughness ($R_q$) values of 1.74 nm, while 1.34 nm for the neat film of PFNT-Cl. The rougher surface of PFNT-F is caused by its stronger aggregation which is consistent with its higher crystallinity as indicated by GIWAXS measurement. More interestingly, both PFNT-F and PFNT-Cl neat films show a fibrous structure. The fibrous morphology has been proven ideal morphology for OSCs, which favors phase separation, charge extraction and transport.[3d, 18] The blend films of PFNT-Cl:N3 and PFNT-F:N3 both exhibit more well-defined fibrous morphology, suggesting excellent morphological compatibility between polymers and N3. The fibrous structure was also observed in their TEM images. Therefore, the favorable morphology formation not only suggests good morphological compatibility between FNT-based polymers and N3, but also well explains their outstanding photovoltaic performance. The natural formation of fibrous morphology both in neat and blend films of the two polymers are probably associated with strong π-π stacking and abundant short interactions of FNT, suggesting FNT is a marvelous building unit and FNT-based polymers are promising donor materials for high-performance OSCs.

10.1002/anie.202215930




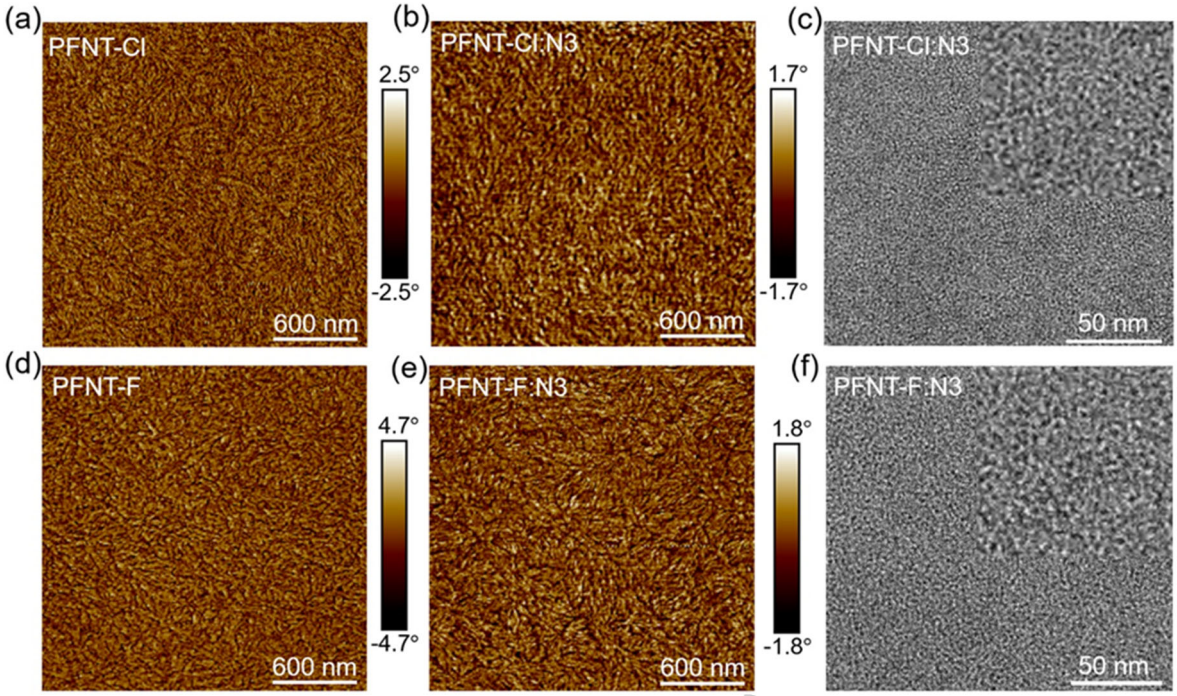


**Figure 4.** The AFM phase image of (a) PFNT-Cl, (b) PFNT-Cl:N3; TEM image of (c) PFNT-Cl:N3; the AFM phase image of (d) PFNT-F, (e) PFNT-F:N3; TEM image of (f) PFNT-F:N3.

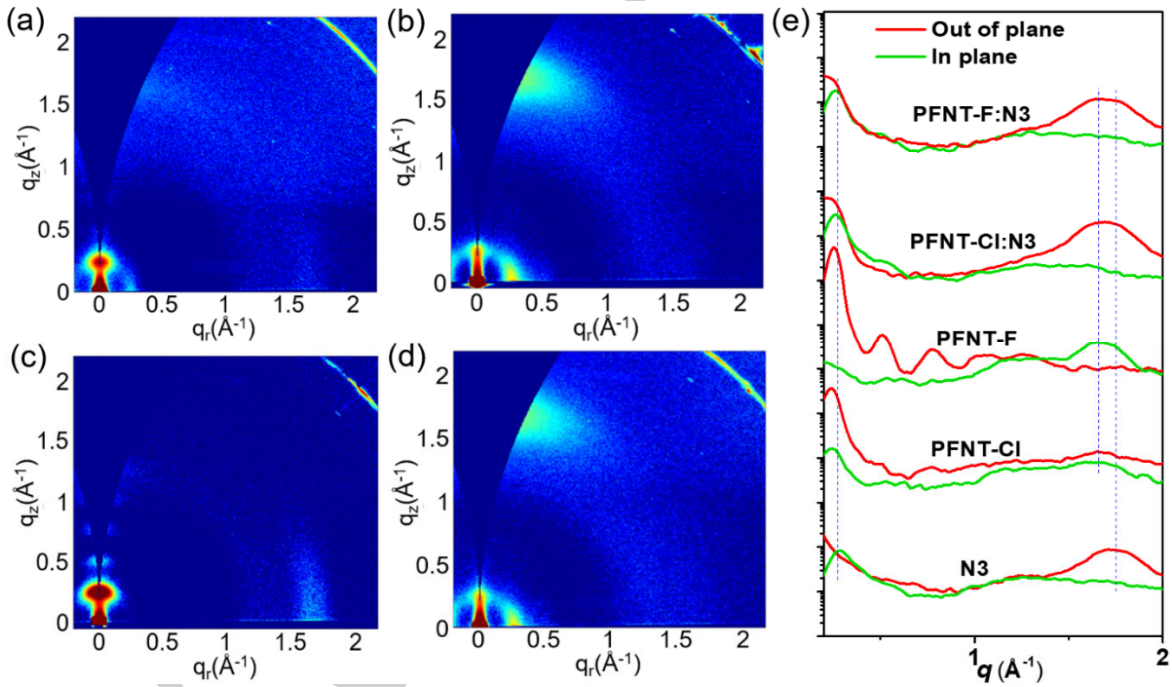


**Figure 5.** The GIWAXS patterns of pure and blend films on PEDOT:PSS-modified Si substrates (a) neat PFNT-Cl, (b) PFNT-Cl:N3, (c) neat PFNT-F, (d) PFNT-F:N3; (e) in-plane and out-of-plane line cuts of pure and blend films.

The grazing-incidence wide-angle X-ray scattering (GIWAXS) measurement was conducted to study the molecular packing information of pure and blend films (Figure 5a-d). The out-of-plane/in-plane line cuts were presented in Figure 5e. The π-π stacking distance and crystal coherence length (CCL) calculated from (010) diffraction peaks were summarized in Table S6, 7. The polymer PFNT-Cl has a π-π stacking distance of 3.78 Å and CCL of 22.39 nm, while those for PFNT-F are 3.76 Å and 25.32 nm. The neat PFNT-F film has out-of-plane diffraction peaks from (100) to (500) while only (100) is observed in neat PFNT-Cl film, suggesting the higher crystallinity and more orderly packed polymer chains of PFNT-F than that of PFNT-Cl which are probably caused by the smaller size of fluorine and strong short interactions between fluorine with other atoms. The diffraction patterns for π-π stacking both in out-of-plane and in-plane direction indicate the mixed edge-on and face-on orientation of PFNT-Cl on PEDOT:PSS substrate. However, the polymer PFNT-F takes an edge-on orientation because it has a π-π

10.1002/anie.202215930





stacking diffraction pattern only in the in-plane direction. Because the PFNT-F/Cl have no glass transition and melting peak in the DSC scan, and their GIWAXS patterns exhibit (100) lamellar peaks and (010) π-π stacking peak, according to the classification of polymers by Harald Ade et al.,[19] the PFNT-Cl/F are orientated ("2D") conjugated amorphous polymers. It should be noted that the benchmark polymer PM6 is also this kind of polymer. [19]

The out-of-plane diffraction peak at 1.75 $Å^{-1}$ and in-plane diffraction peak at 0.27 $Å^{-1}$ for neat N3 film are both overlapped with that of the two polymers, which make it impossible to identify their packing patterns in the blend films. However, we observe a very interesting phenomenon in the blend films. In blend film of PFNT-F:N3, the diffraction peaks from (100) to (500) in out-of-plane direction and π-π stacking diffraction peak in in-plane direction for PFNT-F all disappear, indicating PFNT-F takes a face-on orientation that is totally different from that in neat film. In blend film of PFNT-Cl:N3, the vanishment of π-π stacking diffraction peak of PFNT-Cl in in-plane direction suggests a substantial fraction of PFNT-Cl change from edge-on in neat film to face-on in blend film. The face-on orientation of both polymers in blend film facilitates charge transport and benefits photovoltaic performance. The polymer orientation variations of both polymers are probably caused by the complex interactions between polymers and N3, which also suggests excellent morphological compatibility between FNT-based polymers and N3.

To compare the photovoltaic performance and device stability with the benchmark polymers, we further fabricated the PM6:N3 and D18:N3 based OSCs by using the same electron acceptor N3 and the same device configuration. The highest efficiency of 16.42 % for PM6:N3 and 16.64 % for D18:N3 were obtained (Table S8), which are similar to the efficiency reported in the references. [1c,20] The higher efficiency of PFNT-F/Cl than PM6 and D18 is mainly caused by their impressive FF values of around 0.80, while those for PM6 and D18 are around 0.74. The decent efficiency and remarkable FF value of the FNT-based polymers should be associated with their high and balanced hole/electron mobility, and favorable nanofibrous film morphology. The device stability was measured by placing the completed devices on a hotplate at 60 °C in the nitrogen-filled glovebox and the photovoltaic parameters versus time were recorded in Figure S16 and Table S9-12. After 128 hours, 92.1 % and 90.4% initial PCE were maintained for PFNT-F and PFNT-Cl based OSCs. The polymer PFNT-F has stronger intermolecular interaction with higher crystallinity and shorter π-π stacking distance, which could benefit the morphology stability and should be the reason for its better device stability. [3a, 21] The 87.8 % and 88.2 % initial PCE were maintained for PM6 and D18 based OSCs. It is very clear that the FNT-based polymers also exhibit better device thermal stability than the benchmark polymers PM6 and D18.

## Conclusion

In summary, a new family of multifluorine substituted polymers of PFNT-Cl and PFNT-F was developed from a novel electron-deficient unit FNT. Owing to the solely multifluorine substitutions which withdraw electron by induction, both polymers have low-lying HOMO (~ -5.5 eV) and wide band gap (~ 2.0 eV). Moreover, the complex interactions between polymers and N3 lead to a more well-defined fibrous structure and face-on orientation of both polymers in blend films while mainly edge-on in neat films. The perfectly matched photophysical properties and excellent morphological compatibility enable PFNT-F:N3 and PFNT-Cl:N3 based OSCs to exhibit an efficiency of 17.53 % and 18.10 %, respectively. The slightly higher efficiency of PFNT-Cl based device is mainly attributed to its smaller radiative and non-radiative recombination loss than PFNT-F based device. The PFNT-F based device maintains 92.1 % of initial efficiency after continuous thermal annealing at 60 °C for 128 hours, while that of the PFNT-Cl based device is 90.4 %. The superior thermal stability of PFNT-F should be caused by its shorter π-π stacking distance and higher crystallinity, which suggests enhancing the intermolecular interaction of polymer is an important way to improve the thermal stability of OSCs. This study demonstrates that FNT-based polymers are promising donor materials. It is foreseeable that the FNT unit and multifluorine design strategy are also potentially applicable to developing new semiconducting materials in other organic electronics.

## Acknowledgements

This work was supported by the National Natural Science Foundation of China (22179076), Fund for Zhujiang Young Scholar (18220203), Natural Science Foundation of Guangdong Province (2022A1515011803) and the Department of Education of Guangdong Province (2021KCXTD032).

## Conflict of interest

The authors declare on conflict of interest.

## Data Availability Statement

The synthesis and characterization of monomers and polymers, as well as device fabrication and characterization, including GPC, TGA, UV-vis, CV, AFM and GIWAXS, are provided in the Supporting Information. The supplementary crystallographic data of FNT with CCDC number 2206389 is deposited in the Cambridge Crystallographic Data Centre, which is available free of charge from www.ccdc.cam.ac.uk/data_request/cif.

**Keywords:** Multifluorination • Wide bandgap • Polymer donor • Solar cell

[1] a) C. Li, J. D. Zhou, J. L. Song, J. Q. Xu, H. T. Zhang, X. N. Zhang, J. Guo, L. Zhu, D. H. Wei, G. C. Han, J. Min, Y. Zhang, Z. Q. Xie, Y. P. Yi, H. Yan, F. Gao, F. Liu, Y. M. Sun, *Nat. Energy* **2021**, *6*, 605-613; b) J. Yuan, Y. Q. Zhang, L. Y. Zhou, G. C. Zhang, H. L. Yip, T. K. Lau, X. H. Lu, C. Zhu, H. J. Peng, P. A. Johnson, M. Leclerc, Y. Cao, J. Ulanski, Y. F. Li, Y. P. Zou, *Joule* **2019**, *3*, 1140-1151; c) K. Jiang, Q. Y. Wei, J. Y. L. Lai, Z. X. Peng, H. Kim, J. Yuan, L. Ye, H. Ade, Y. P. Zou, H. Yan, *Joule* **2019,** *3*, 3020-3033; d) Y. H. Liu, B. W. Li, C. Q. Ma, F. Huang, G. T. Feng, H. Z. Chen, J. H. Hou, L. P. Yan, Q. Y. Wei, Q. Luo, Q. Y. Bao, W. Ma, W. Liu, W. W. Li, X. J. Wan, X. T. Hu, Y. C. Han, Y. W. Li, Y. H. Zhou, Y. P. Zou, Y. W. Chen, Y. F. Li, Y. S. Chen, Z. Tang, Z. C. Hu, Z. G. Zhang, Z. S. Bo, *Sci. China: Chem.* **2022**, *65*, 224-268; e) S. X. Li, C. Z. Li, M. M. Shi, H. Z. Chen, *ACS Energy Lett.* **2020**, *5*, 1554-1567; f) X. L. Kong, C. Zhu, J. Y. Zhang, L. Meng, S. C. Qin, J. Q. Zhang, J. Li, Z. X. Wei, Y. F. Li, *Energy Environ. Sci.* **2022**, *15*, 2011-2020; f) Y. A. Wei, Z. H. Chen, G. Y. Lu, N. Yu, C. Q. Li, J. H. Gao, X. B. Gu, X. T. Hao, G. H. Lu, Z. Tang, J.

10.1002/anie.202215930




Q. Zhang, Z. X. Wei, X. Zhang, H. Huang, *Adv. Mater.* **2022**, *34*, 2204718; g) J. H. Gao, N. Yu, Z. J. Chen, Y. N. Wei, C. Q. Li, T. H. Liu, X. B. Gu, J. Q. Zhang, Z. X. Wei, Z. Tang, X. T. Hao, F. J. Zhang, X. Zhang, H. Huang, *Adv. Sci.* **2022**, *9*, 2203606

[2] a) H. Fu, Z. Wang, Y. Sun, *Angew. Chem., Int. Ed.* **2019**, *58*, 4442-4453; b) G. Zhang, H. Ning, H. Chen, Q. Jiang, J. Jiang, P. Han, L. Dang, M. Xu, M. Shao, F. He, Q. Wu, *Joule* **2021**, *5*, 931-944; c) Y. Huang, E. J. Kramer, A. J. Heeger, G. C. Bazan, *Chem. Rev.* **2014**, *114*, 7006-7043; d) H. L. Sun, T. Liu, J. W. Yu, T. K. Lau, G. Y. Zhang, Y. J. Zhang, M. Y. Su, Y. M. Tang, R. J. Ma, B. Liu, J. E. Liang, K. Feng, X. H. Lu, X. G. Guo, F. Gao, H. Yan, *Energy Environ. Sci.* **2019**, *12*, 3328-3337; e) C. G. Li, X. Z. Chen, X. Han, N. Yu, Y. Wei, J. Gao, H. Chen, M. Zhang, A. Wang, J. Zhang, Z. Wei, Q. Peng, Z. Tang, X. Hao, X. Zhang, H. Huang, *J. Am. Chem. Soc.* **2022**, *144*, 14731-14739; f) S. T. Pang, Z. Q. Wang, X. Y. Yuan, L. H. Pan, W. Y. Deng, H. R. Tang, H. B. Wu, S. S. Chen, C. H. Duan, F. Huang, Y. Cao, *Angew. Chem., Int. Ed.* **2021**, *60*, 8813-8817.

[3] a) Q. J. Jiang, P. W. Han, H. J. Ning, J. Q. Jiang, H. Chen, Y. H. Xiao, C. R. Ye, J. M. Chen, M. Lin, F. He, X. C. Huang, Q. H. Wu, *Nano Energy* **2022,** *101*, 107611; b) Q. S. Liu, Y. F. Jiang, K. Jin, J. Q. Qin, J. G. Xu, W. T. Li, J. Xiong, J. F. Liu, Z. Xiao, K. Sun, S. F. Yang, X. T. Zhang, L. M. Ding, *Sci. Bull.* **2020**, *65*, 272-275; c) J. Wu, G. Li, J. Fang, X. Guo, L. Zhu, B. Guo, Y. Wang, G. Zhang, L. Arunagiri, F. Liu, H. Yan, M. Zhang, Y. Li, *Nat. Commun.* **2020**, *11*, 4612; d) L. Zhu, M. Zhang, J. Xu, C. Li, J. Yan, G. Zhou, W. Zhong, T. Hao, J. Song, X. Xue, Z. Zhou, R. Zeng, H. Zhu, C.-C. Chen, R. C. I. MacKenzie, Y. Zou, J. Nelson, Y. Zhang, Y. Sun, F. Liu, *Nat. Mater.* **2022,** *21*, 656-663.

[4] a) F. Meng. L. H. Li, M. Zhang, Z. G. Zhang, D. B. Zhao, *Angew. Chem. Int. Ed.* **2022**, *61*, e202206311; b) H. Zhou, L. Yang, A. C. Stuart, S. C. Price, S. Liu, W. You, *Angew. Chem., Int. Ed.* **2011**, *50*, 2995-2998; c) S. Holliday, Y. L. Li, C. K. Luscombe, *Prog. Polym. Sci.* **2017**, *70*, 34-51; d) K. Q. He, P. Kumar, Y. Yuan, Y. N. Li, *Mater. Adv.* **2021**, *2*, 115-145; e) P. W. Han, M. Lin, Q. J. Jiang, H. J. Ning, M. B. Su, L. Dang, F. He, Q. H. Wu, *CCS Chem.* **2022**, *4*, DOI: 10.31635/ccschem.022.202201839.

[5] a) Y. Y. Liang, D. Q. Feng, Y. Wu, S. T. Tsai, G. Li, C. Ray, L. P. Yu, *J. Am. Chem. Soc.* **2009**, *131*, 7792-7799; b) S. H. Liao, H. J. huo, Y. S. Cheng, S. A. Chen, *Adv. Mater.* **2013**, *25*, 4766-4771.

[6] a) M. J. Zhang, X. Guo, W. Ma, H. Ade, J. H. Hou, *Adv. Mater.* **2015**, *27*, 4655-4660; b) Y. Ie, J. M. Huang, Y. Uetani, M. Karakawa, Y. Aso, *Macromolecules* **2012**, *45*, 4564-4571.

[7] L. Lu, T. Zheng, Q. Wu, A. M. Schneider, D. Zhao, L. Yu, *Chem. Rev.* **2015**, *115*, 12666-12731.

[8] a) J. Wu, C.-Y. Liao, Y. Chen, R. M. Jacobberger, W. Huang, D. Zheng, K.-W. Tsai, W.-L. Li, Z. Lu, Y. Huang, M. R. Wasielewski, Y.-M. Chang, T. J. Marks, A. Facchetti, *Adv. Energy Mater.* **2021**, *11*, 2102648; b) J. E. Liang, M. G. Pan, G. D. Chai, Z. X. Peng, J. Q. Zhang, S. W. Luo, Q. Han, Y. Z. Chen, A. Shang, F. J. Bai, Y. Xu, H. Yu, J. Y. L. Lai, Q. Chen, M. J. Zhang, H. Ade, H. Yan, *Adv. Mater.* **2020**, *32*, 2003500; c) C. K. Sun, F. Pan, S. S. Chen, R. Wang, R. Sun, Z. Y. Shang, B. B. Qiu, J. Min, M. L. Lv, L. Meng, C. F. Zhang, M. Xiao, C. D. Yang, Y. F. Li, *Adv. Mater.* **2019**, *31*, 1905480; d) X. F. Liao, L. Zhang, X. T. Hu, L. Chen, W. Ma, Y. W. Chen, *Nano Energy* **2017**, *41*, 27-34; e) S. Albrecht, S. Janietz, W. Schindler, J. Frisch, J. Kurpiers, J. Kniepert, S. Inal, P. Pingel, K. Fostiropoulos, N. Koch, D. Neher, *J. Am. Chem. Soc.* **2012**, *134*, 14932-14944; f) W. T. Li, Q. S. Liu, K. Jin, M. Cheng, F. Hao, W. Q. Wu, S. J. Liu, Z. Xiao, S. F. Yang, S. W. Shi, L. M. Ding, *Mater. Chem. Front.* **2020**, *4*, 1454-1458; g) C. K. Sun, F. Pan, H. J. Bin, J. Q. Zhang, L. W. Xue, B. B. Qiu, Z. X. Wei, Z. G. Zhang, Y. F. Li, *Nat. Commun.* **2018**, *9*, 743; h) Y. Liu, J. Zhao, Z. Li, C. Mu, W. Ma, H. Hu, K. Jiang, H. Lin, H. Ade, H. Yan, *Nat. Commun.* **2014**, *5*, 5293; i) S. C. Price, A. C. Stuart, L. Q. Yang, H. X. Zhou, W. You, *J. Am. Chem. Soc.* **2011**, *133*, 4625;

[9] Q. T. Zhang, J. M. Tour, *J. Am. Chem. Soc.* **1998**, *120*, 5355-5362

[10] a) S. J. Ko, Q. V. Hoang, C. E. Song, M. A. Uddin, E. Lim, S. Y. Park, B. H. Lee, S. Song, S. J. Moon, S. Hwang, P. O. Morin, M. Leclerc, G. M. Su, M. L. Chabinyc, H. Y. Woo, W. S. Shin, J. Y. Kim, *Energy Environ. Sci.* **2017**, *10*, 1443-1455; b) J. Liu, L. K. Ma, Z. K. Li, H. W. Hu, F. K. Sheong, G. Y. Zhang, H. Ade, H. Yan, *J. Mater. Chem. A* **2018**, *6*, 23270-23277; c) X. F. Liao, F. Y. Wu, Y. K. An, Q. Xie, L. Chen, Y. W. Chen, *Macromol. Rapid. Comm.* **2017**, *38*, 1600556.

[11] a) H. J. Son, W. Wang, T. Xu, Y. Y. Liang, Y. E. Wu, G. Li, L. P. Yu, *J. Am. Chem. Soc.* **2011**, *133*, 1885-1894; b) X. Zhang, J. P. Wu, D. H. Wei, Y. H. Cai, X. B. Sun, *Dyes Pigm.* **2021**, *187*, 109109.

[12] a) J. Cornil, D. A. dos Santos, X. Crispin, R. Silbey, J. L. Bre´das *J. Am. Chem. Soc.* **1998**, *120*, 1289-1299; b) S. Varghese, S. Das, *J. Phys. Chem. Lett.* **2011**, *2*, 863-873.

[13] F. Panzer, H. Bässler, A. Köhler, *J. Phys. Chem. Lett.*, **2017**, *8*, 114–125

[14] X. L. Kong, J. Zhang, L. Meng, C. K. Sun, S. C. Qin, C. Zhu, J. Q. Zhang, J. Li, Z. X. Wei, Y. F. Li, *CCS Chem.* **2022**, *4*, DOI: 10.31635/ccschem.022.202202056.

[15] a) V. D. Mihailetchi, L. J. A. Koster, J. C. Hummelen, P. W. M. Blom, *Phys. Rev. Let.* **2004**, *93*, 216601; b) L. Y. Lu, T. Xu, W. Chen, J. M. Lee, Z. Q. Luo, I. H. Jung, H. I. Park, S. O. Kim, L. P. Yu, *Nano Lett.* **2013**, *13*, 2365-2369.

[16] L. J. A. Koster, V. D. Mihailetchi, H. Xie, P. W. M. Blom, *Appl. Phys. Lett.* **2005**, *87*, 203502.

[17] a) Y. M. Wang, D. P. Qian, Y. Cui, H. T. Zhang, J. H. Hou, K. Vandewal, T. Kirchartz, F. Gao, *Adv. Energy Mater.* **2018**, *8*, 1801352; b) D. P. Qian, Z. L. Zheng, H. F. Yao, W. Tress, T. R. Hopper, S. L. Chen, S. S. Li, J. Liu, S. S. Chen, J. B. Zhang, X. K. Liu, B. W. Gao, L. Q. Ouyang, Y. Z. Jin, G. Pozina, I. A. Buyanova, W. M. Chen, O. Inganas, V. Coropceanu, J. L. Bredas, H. Yan, J. H. Hou, F. L. Zhang, A. A. Bakulin, F. Gao, *Nat. Mater.* **2018**, *17*, 703-709.

[18] a) T. Liu, L. Huo, S. Chandrabose, K. Chen, G. Han, F. Qi, X. Meng, D. Xie, W. Ma, Y. Yi, J. M. Hodgkiss, F. Liu, J. Wang, C. Yang, Y. Sun, *Adv. Mater.* **2018**, *30*, 1707353; b) K. Chong, X. Xu, H. Meng, J. Xue, L. Yu, W. Ma, Q. Peng, *Adv. Mater.* **2022**, *34*, 2109516.

[19] Z. X. Peng, L. Ye, H. Ade, arXiv:2005.13155.

[20] D. H. Li, C. H. Guo, X. Zhang, B. C. Du, C. Yu, P. Wang, S. L. Cheng, L. Wang, J. L. Cai, H. Wang, D. Liu, H. F. Yao, Y. M. Sun, J. H. Hou, T. Wang, *Sci. China. Chem.* **2022**, *65*, 373-381.

[21] a) X. Li, L. Zhou, X. Lu, L. Cao, X. Du, H. Lin, C. Zheng, S. Tao, *Mater. Chem. Front.* **2021**, *5*, 3850-3858; b) W. Li, D. Liu, T. Wang, *Adv. Funct. Mater.* **2021**, *31*, 2104552.

10.1002/anie.202215930

WILEY-VCH

RESEARCH ARTICLE

## Entry for the Table of Contents

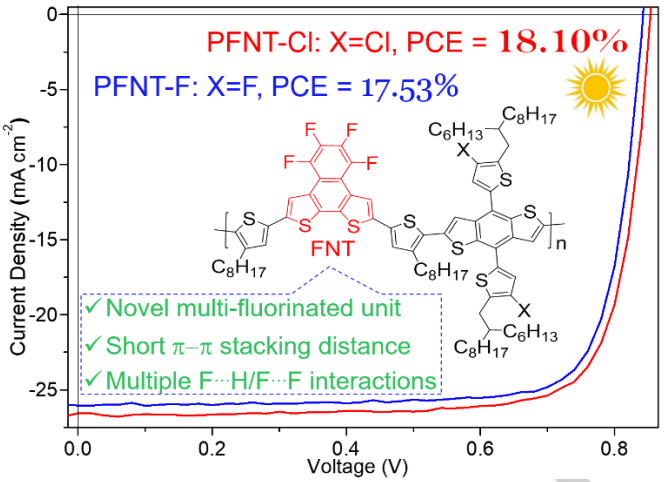


An electron-deficient tetrafluoronaphthodithiophene (FNT) was created to construct a family of PFNT-F/Cl polymers for organic solar cells. The PFNT-F/Cl-based OSCs exhibit impressive FF values of 0.80, and remarkable PCEs of 17.53 % and 18.10 %, suggesting multifluorinated polymers are promising donor materials for non-fullerene OSCs.